

# PHYSICAL REVIEW D

## PARTICLES AND FIELDS

THIRD SERIES, VOLUME 42, NUMBER 2

15 JULY 1990

### Search for $> 200$ TeV photons from Cygnus X-3 in 1988 and 1989

D. Ciampa, K. Green, J. Kolodziejczak, J. Matthews, D. Nitz, D. Sinclair,  
G. Thornton,\* and J. C. van der Velde  
*University of Michigan, Ann Arbor, Michigan 48109*

G. L. Cassiday,<sup>†</sup> R. Cooper, S. C. Corbato, B. R. Dawson, J. W. Elbert,<sup>‡</sup> B. E. Fick,  
D. B. Kieda, S. Ko, D. F. Liebing, E. C. Loh, M. H. Salamon, J. D. Smith,  
P. Sokolsky, S. B. Thomas, and B. Wheeler  
*University of Utah, Salt Lake City, Utah 84112*

(Received 17 January 1990)

Over a period of 16 months from April 1988 to August 1989, we have monitored the flux of cosmic-ray showers with energies above  $2 \times 10^{14}$  eV. We used a two-level array of scintillators covering an area of  $3 \times 10^4$  m<sup>2</sup>. Counters on the surface measure the size and direction of each shower while counters buried 3 m beneath the surface sample the muons. By selecting showers with relatively few muons (less than one-tenth the average) the background of hadron-induced showers should be reduced by a factor of 150 or more while showers started by  $\gamma$  rays should not be affected by this cut. We find no evidence for an excess from the direction of Cygnus X-3 either in ordinary showers or in muon-poor showers. For energies above  $2 \times 10^{14}$  eV, with 90% confidence, we find the excess flux of cosmic rays from the direction of Cygnus X-3 to be less than  $1.3 \times 10^{-13}$  cm<sup>-2</sup>s<sup>-1</sup> and the flux of photons (assuming they produce muon-poor showers) to be less than  $1.5 \times 10^{-14}$  cm<sup>-2</sup>s<sup>-1</sup>. This limit is substantially below the level of signals reported by earlier work. The period of observation included the intense radio bursts of June and July 1989. A portion of the data covering the 77-day period surrounding these events also showed no evidence for an excess.

#### I. INTRODUCTION

The x-ray binary system Cygnus X-3 has been the object of intense study and the subject of much controversy for more than a decade.<sup>1</sup> It was discovered as an x-ray source in 1967 and thereafter the emission was found to be modulated with a very stable period of 4.79 h. But at energies beyond the hard x-ray region ( $\sim 80$  keV) the measurements become controversial. A group<sup>2</sup> using data from the SAS-2  $\gamma$ -ray telescope reported the detection of a modulated signal in the 1 MeV to 1 GeV region, but later observations<sup>3,1</sup> using data from the COS-B satellite did not confirm this result. However, another group<sup>4</sup> using COS-B data *do* see evidence for a  $\gamma$ -ray source. In the very-high-energy region ( $E \gtrsim 10^{12}$  eV), experimenters have used mirrors pointed at Cygnus X-3 to collect Cherenkov light from showers produced by cosmic rays in the upper atmosphere. Several groups<sup>5-9</sup> have reported signals in this energy region but all have relied on the 4.79-h modulation to extract their signals from the background of cosmic rays, and in no case is the statistical significance of the result beyond question.

In the energy range accessible to ground arrays at sea level ( $> 10^{15}$  eV) the first reported observation of Cygnus X-3 was by Samorski and Stamm.<sup>10</sup> This was followed by other observations<sup>11,12</sup> in which the source was seen with substantially lower intensity and only after phase analysis was used to extract the signal from the cosmic-ray background. Working at higher elevation, and therefore lower energy, the array at Ooty<sup>13</sup> found a signal in ordinary showers which was enhanced by the use of phase analysis, while the Cygnus Array<sup>14</sup> found no evidence for a signal in either ordinary showers or muon-poor showers. But at a much higher energy a group using the Fly's Eye detector,<sup>15</sup> and another group using the large ground array at Akeno,<sup>16</sup> reported signals which were observed without the use of phase analysis. On the other hand, a group using the array at Haverah Park<sup>17</sup> and the Akeno group<sup>18</sup> working at somewhat lower energy found no evidence for such a signal. These results are summarized in Table I.

The radiation from Cygnus X-3 is often compared to a power spectrum<sup>1,11</sup> in which the integral flux varies inversely as the first power of the energy. If this were the case, the numbers in the last column of Table I would be

TABLE I. Summary of the published results on the flux of ultra-high-energy neutral radiation from Cygnus X-3. The fluxes are time-averaged integrals above the stated energy.

| Reference       | Period of exposure | Energy (10 <sup>15</sup> eV) | Flux (10 <sup>-15</sup> cm <sup>-2</sup> s <sup>-1</sup> ) | Energy × Flux (eV cm <sup>-2</sup> s <sup>-1</sup> ) |
|-----------------|--------------------|------------------------------|--|--|
| 10              | 3/76→1/80          | 2                            | 74±32  | 148±64   |
| 11 <sup>a</sup> | 1/78→1/83          | 3                            | 15±3   | 45±9   |
| 12 <sup>b</sup> | 1/81→9/84          | 1                            | 11±4   | 11±4   |
| 13              | 6/84→11/86         | 0.25                         | 716±315  | 179±78   |
| 14 <sup>c</sup> | 4/86→5/87          | 0.05                         | < 76   | < 3.8  |
| 15              | 11/81→5/88         | 500                          | 0.02±0.006   | 10±3   |
| 16              | 12/84→7/89         | 500                          | 0.018±0.007  | 9±3.5  |
| 17 <sup>d</sup> | 1/74→7/88          | 500                          | < 0.008  | < 4  |
| 18              | 10/81→10/86        | 150                          | < 0.031  | < 4.6  |

<sup>a</sup>Signal seen only after phase analysis.

<sup>b</sup>Signal seen only after phase analysis on muon-poor shower.

<sup>c</sup>Quoted limit is for showers with no observed muons in a 44-m<sup>2</sup> muon detector.

<sup>d</sup>Quoted limit is for  $\gamma$  rays. Limit for neutrons is factor 2 lower.

constant. However, one problem with observing Cygnus X-3 is that the source may be variable. Certainly it is known to have sporadic outbursts in the radio, infrared, and soft x-ray regions of the spectrum. During these flares the radio intensity may change by as much as two orders of magnitude. On the other hand, a search for  $\gamma$  rays above 10<sup>14</sup> eV around the time of the radio outbursts of June and July 1989 did not reveal the source,<sup>19</sup> even though such  $\gamma$  rays were reported at the time of previous radio outbursts.<sup>20</sup> In all the experiments at energies above and hard x-ray region, experimentors have had to extract a signal which is only a few standard deviations above the background of cosmic rays. The large variations shown by the data in Table I may be due to changes in the intensity of the source. On the other hand, the apparent signal may be nothing more than statistical fluctuations in the cosmic-ray background.

In this experiment we measure separately the electron and muon components of showers. Muons are produced copiously in hadronic air showers but are relatively rare in  $\gamma$ -ray-induced air showers. By cutting on the number of muons we reduce the background of cosmic rays by a factor of 150 or more. The technique is not new. It has been used by the groups working at Akeno<sup>12</sup> and Los Alamos.<sup>14</sup> In our case, however, the area of muon counters is much greater (more than five times greater). A large area of muon counters is important because ultimately the ability of this technique to select showers induced by photons from a large background of showers induced by hadrons is limited by downward fluctuations in the number of muons detected.

## II. DESCRIPTION OF THE ARRAY

The array is located at Dugway, Utah (40°N, 113°W, 870 g/cm<sup>2</sup>). It consists of 33 counter stations on the surface distributed within a circle of 100-m radius, and 8

patches of counters buried 3 m below the surface. There are four inner patches, each ~50 m from the center of the array and four outer patches ~110 m from the center. The counters on the surface measure the size and direction of each shower while the buried counters sample the muons. A counter station on the surface has an area of 1.5 m<sup>2</sup> and consists of four slabs of scintillator each viewed by two photomultiplier tubes (PMT's). A patch of buried counters contains 64 sheets of scintillator, each 2.5 m<sup>2</sup> in area and viewed by a single 5-in. PMT at its center. Measurements taken with overlapping scintillators showed that the buried counters detected muons with an efficiency of 93%.<sup>21</sup> The total area of buried counters is 1280 m<sup>2</sup>.

Counter stations on the surface sample the density of particles in the shower and measure the arrival times of various pieces of the shower to an accuracy of  $\pm 1$  ns. The direction of the shower is first computed approximately from these times by fitting the shower front to a plane. Next, the size of the shower and the location of its core are determined by fitting the sampled particle densities to the lateral distribution function for electrons given by Greisen.<sup>22</sup> Finally, the direction of the shower is recalculated by fitting the shower front to a cone whose apex is at the core.

The directional resolution  $\delta\theta$  is defined such that 72% of events from a point source will reconstruct within  $\delta\theta$  of the source direction. This definition maximizes  $S/\sqrt{B}$  for a signal  $S$  in the presence of a uniform background  $B$ . It is measured in two ways. In one technique the array is divided into two parts by assigning alternate surface counters to each part and computing the direction of the shower separately for each half. The difference divided by 2 is an estimate of  $\delta\theta$  for the whole array. The accuracy of this method may be vulnerable to correlated errors; consequently we also employ an independent technique which uses four tracking air-Cherenkov telescopes which

surround the array. Some showers are detected by both instruments and the angle between the two directions is a measure of the combined error of the two devices.

Both methods yield similar results. For cores within 100 m of the center of the array and  $N_e > 10^4$ ,  $\delta\theta = 3^\circ$ . Furthermore, the Cherenkov telescope comparisons indicate that systematic pointing error is negligible.

### III. MUON CONTENT OF SHOWERS

The muons associated with each shower are sampled by the buried counters. We use the core position and shower direction determined by the surface array and fit the data from the buried counters to the lateral distribution function for muons given by Greisen.<sup>23</sup> The outer four patches of muon counters were brought on line during the first half of the run. By January 1989 all eight patches were operating. The muon counters do not record pulse height so the method used to estimate the number of muons in the shower allows for the possibility of several hits in each counter. The time window for accepting pulses from the muon counters is  $\pm 55$  ns for the inner four patches and  $\pm 100$  ns for the outer four, relative to the arrival time of the shower front at the buried counters as determined by the surface array. Our measurements show that the average number of muons associated with a shower depends on its size  $N$ , and zenith angle  $\theta$ , in the following way:

$$\langle \log_{10} N_\mu \rangle = a + b \sec\theta + c \log_{10} N \quad (1)$$

for values of  $N$  between  $3 \times 10^4$  and  $10^6$ . The coefficients in expression (1) are determined from the calibration of

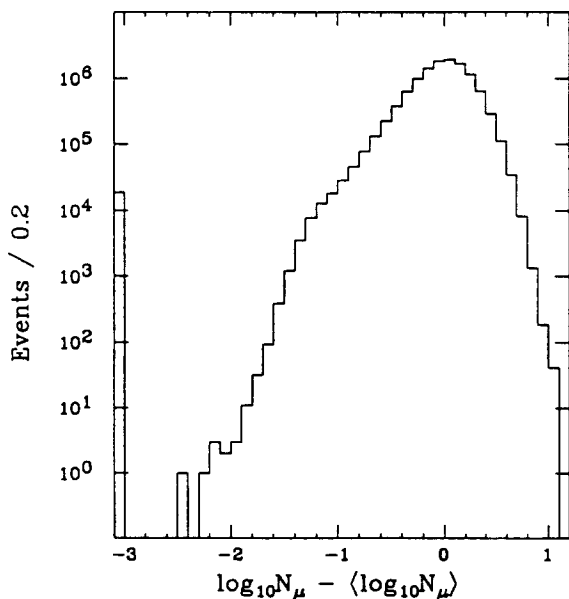


FIG. 1. The dispersion in the number muons associated with a shower. The average quantity  $\langle \log_{10} N_\mu \rangle$  for a shower of size  $N$  is determined using the empirical relation given in Eq. (1). The figure contains  $1.2 \times 10^7$  showers of which  $2 \times 10^4$  have no recorded muons and are put into the underflow bin.

each data set. Average values for  $a$ ,  $b$ , and  $c$  are  $-0.98$ ,  $0.62$ , and  $0.82$ , respectively. The dependence on zenith angle arises because the electron and muon components of the shower develop differently as the shower progresses. Shower simulations<sup>22</sup> show that for showers of a given energy, the number of electrons decreases rapidly with increasing zenith angle while the number of muons decreases relatively slowly.

Relation (1) is used to determine the expected number of muons for each shower. If the measured number of muons is less than 10% of the expected number, the shower is said to be "muon poor." Our simulations of the muon and electron content of air showers indicate that cutting showers with less than one-tenth the expected number of muons should retain  $\geq 98\%$  of showers induced by  $\gamma$  rays. Such a cut applied to the data reduces the number of showers by a large factor which increases with shower size. For showers with  $3 \times 10^4 < N < 10^5$  it is  $\sim 150$  while for  $N > 10^5$  it is  $\sim 700$ . The distribution of  $N_\mu$  relative to  $\langle N_\mu \rangle$  is shown in Fig. 1. (We define  $\langle N_\mu \rangle \equiv 10^{\langle \log_{10} N_\mu \rangle}$ .)

### IV. RESPONSE TO PHOTONS FROM A CELESTIAL SOURCE

To measure the flux from a source, or to set a limit, we need to know the function  $A(E, t)$ , which is the acceptance of the array for photons from the source. It is a function of  $E$ , the energy of the photon and  $t$ , the time of day. As the source rises and sets the solid angle subtended by the array changes. In addition, the efficiency of the array depends on the energy of the shower because small showers (i.e., low-energy showers) are less likely to trigger the array than large showers. We impose a small size cutoff at  $3 \times 10^4$  particles and a large size cutoff at  $10^6$  particles. The thickness of atmosphere between the array and the source changes as the source rises and sets; thus showers of a given energy arrive at different stages of development requiring that the relation between shower size and energy be changed with the zenith angle of the source. Also, fluctuations in shower development smear this relation so that even at a fixed zenith angle there is not a direct correspondence between size and energy but a spectrum of energies whose shape depends on the fluctuations in shower development. Taking account of all these effects, we obtain the response curve shown in Fig. 2. It represents the acceptance of the array, with the imposed cuts on shower size, for a flat ( $dI/dE = \text{const}$ ) energy spectrum of photons coming from the direction of Cygnus X-3.

The derivation of the function shown in Fig. 2 involved the following. First we measured how the trigger efficiency of the array depends on the size of the shower by comparing the measured size spectrum of showers which trigger the array with a spectrum of the form

$$\frac{dI}{d(\log N)} \propto N^{-\alpha}.$$

This comparison is shown in Fig. 3, with  $\alpha = 1.5$ . For showers with  $7 \times 10^4 < N < 10^6$  this spectrum fits the data well. Below  $7 \times 10^4$  the data fall short of this spectrum

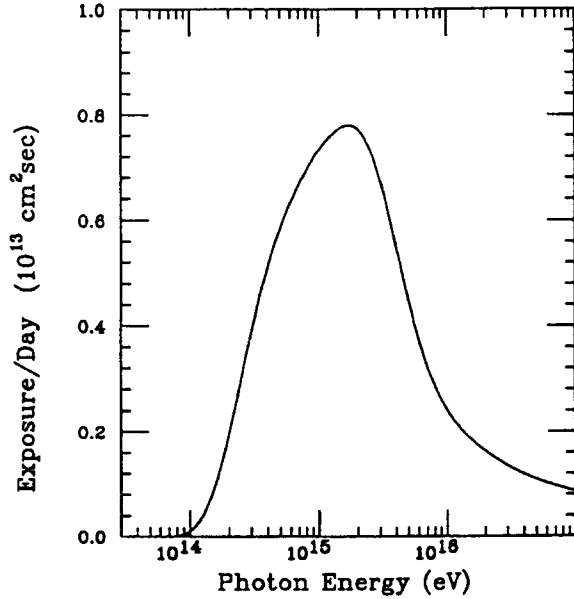


FIG. 2. The calculated daily exposure of the array to a flat energy spectrum of photons from the direction of Cygnus X-3. Included are cuts on shower size,  $3 \times 10^4 < N < 10^6$  and core location,  $< 100$  m from the center of the array.

and we take the difference to be a measure of the inefficiency of our trigger for small showers. At  $N = 3 \times 10^4$  the efficiency is 0.5 and we impose our small size cut at this value. For  $N > 10^6$  we impose our large size cut because the measurement of shower size becomes more uncertain due to saturation of the counters. In addition to its dependence on the size of the shower, the acceptance of the array also depends on the direction of the

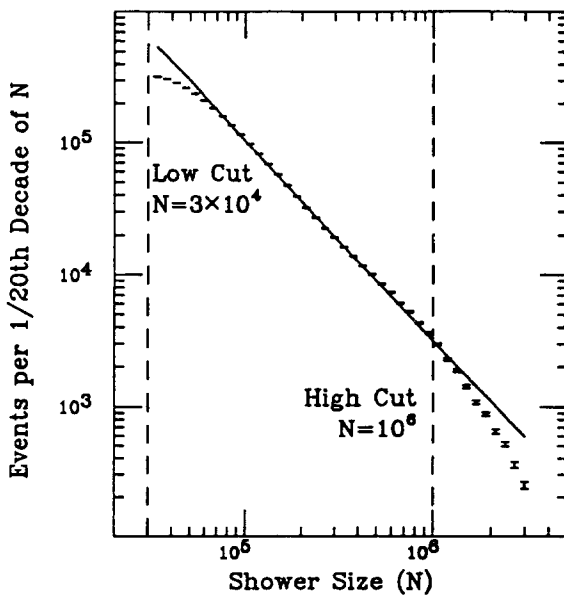


FIG. 3. The measured size spectrum of showers which trigger the array.

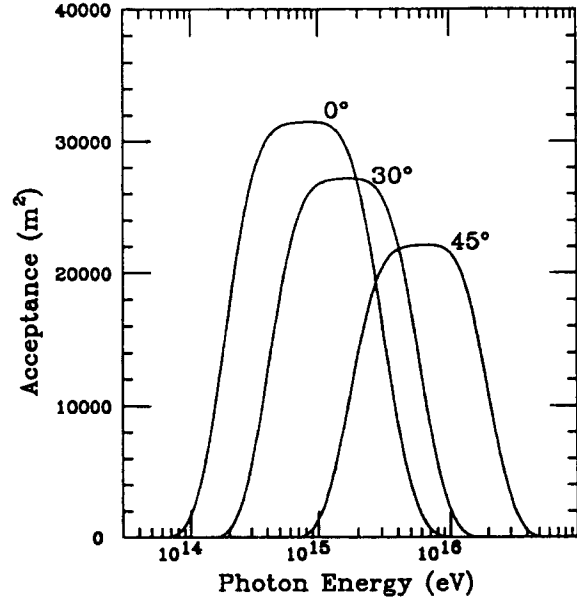


FIG. 4. The calculated acceptance of the array, after cuts on shower size, for showers induced by  $\gamma$  rays from a celestial source. The acceptance depends on the energy of the  $\gamma$  ray and the zenith angle of the source. The curves are for showers whose cores lie within 100 m of the center of the array and have sizes between  $3 \times 10^4$  and  $10^6$  particles.

shower because the solid angle subtended by the array varies as the cosine of the zenith angle of the source.

The next step is to change the acceptance of the array from a function of shower size and zenith angle to a function of energy of the primary photon and its zenith angle. To this end, we used a relation derived from the simulations of Fenyves *et al.*<sup>24</sup> to convert the number of electrons in a shower, and the depth (in radiation lengths) of atmosphere, to the energy of the primary photon. Thus we obtained the central value of energy for a given size of shower and zenith angle. However, the development of a shower is subject to fluctuations in the number of electrons. We estimated these with our own calculations of shower development. The result is shown in the curves of Fig. 4, which give the acceptance of the array as a function of the energy of the primary photon for different zenith angles of the source.

For the final step we use these curves along with the path of the source across the sky to generate the function shown in Fig. 2. This function is the integral over time of the acceptance  $A(E, t)$  for photons from the source as it moves across the sky. It is the response function of the array and we use it in combination with a hypothesized shape for the energy spectrum to measure (or obtain a limit on) the flux of photons from Cygnus X-3.

#### V. RESPONSE OF THE ARRAY TO PHOTONS FROM CYGNUS X-3

We represent the differential energy spectrum of photons from the source by a power law. Following Gould and Schröder<sup>25</sup> we modify this to account for absorption

of these photons by photons of the 3-K blackbody radiation in traveling the 11-kpc distance between Cygnus X-3 and Earth. Thus the number of photons, with energies between  $E$  and  $E + dE$ , detected by the array, is given by

$$dN_\gamma = KE^{-\beta} f(E) \int_0^T A(E, t) dt dE . \quad (2)$$

Here  $f(E)$  is the fraction of photons of energy  $E$  not absorbed by the blackbody radiation and  $K$  and  $\beta$  are constants. The function  $f(E)$  has the value of 1.0 for energies below  $1.6 \times 10^{14}$  eV. It drops to a minimum of 0.25 at  $E = 2 \times 10^{15}$  eV and rises to  $\sim 0.5$  at  $E = 10^{16}$  eV.

The function  $dN_\gamma/dE$  is plotted in Fig. 5 for the value  $\beta=2$ . It is useful to define a quantity  $A_{\text{eff}}$ , the effective area of the array for the source Cygnus X-3. Roughly speaking it is the actual area of the array reduced by two factors: the fraction of time the source is in a position to shine on the array and the efficiency of the array. Precisely, it is defined as

$$TA_{\text{eff}} \int_{E'}^\infty KE^{-\beta} f(E) dE \equiv \int_0^\infty KE^{-\beta} f(E) \int_0^T A(E, t) dt dE . \quad (3)$$

Here  $T$  is the duration of the exposure and  $E'$  is the energy at which the array becomes sensitive to showers. Since the response function of the array (Fig. 2) turns on rather slowly, the choice of  $E'$  is somewhat arbitrary and the result of our measurement of flux does not depend on the choice. What we measure, or set a limit on, is the scale of an assumed differential energy spectrum which is then expressed as a point on the corresponding integral spectrum. Though the placement of this point is some-

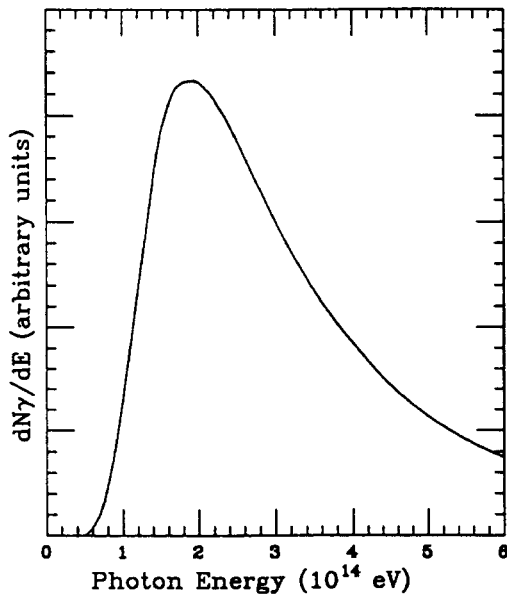


FIG. 5. The calculated differential energy spectrum of showers that would be detected by the array if the incident spectrum were of the form  $dI/dE \propto f(E)E^{-2}$  and the response of the array were as shown in Fig. 2. The function  $f(E)$  represents the fraction of photons not absorbed by the 3-K blackbody radiation.

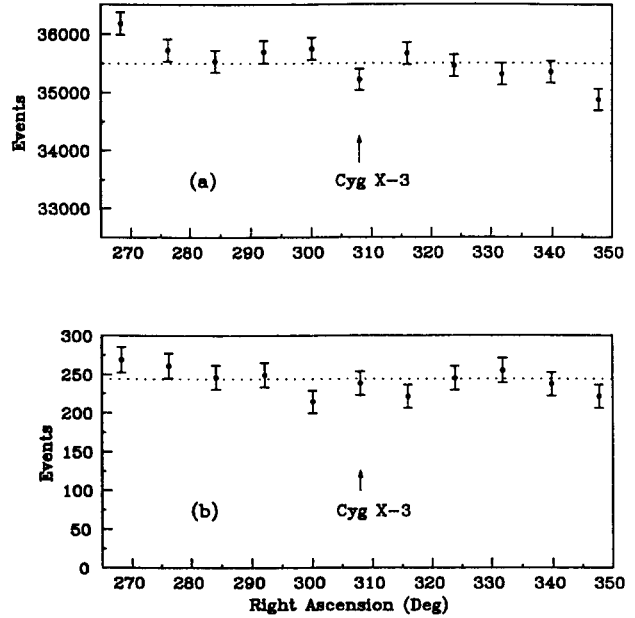


FIG. 6. The distributions in the celestial reference frame of showers which pass our cuts and come from a strip of declination  $\pm 3^\circ$  centered on the declination of Cygnus X-3. The middle bin in each case contains showers in a  $3^\circ$  radius circle centered on the RA of Cygnus X-3. The horizontal line is the average of the 10 circles adjacent to the central bin. (a) contains all showers; (b) contains those whose muon content is less than 10% of the average.

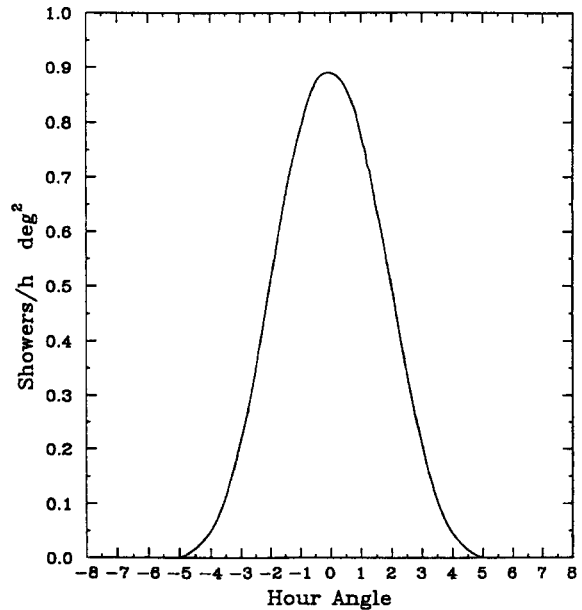


FIG. 7. In the local horizontal reference frame, this is the rate of showers along an annular strip  $\pm 3^\circ$  centered on  $40.9^\circ$ , the declination of Cygnus X-3. The backgrounds for data sets of relatively short duration are calculated by integrating the contributions from each of the elements of hour angle weighted by the detector's on-time when Cygnus X-3 is at that hour angle.

TABLE II. Showers coming from the direction of Cygnus X-3 are tabulated according to their muon content. The data were recorded between April 1988 and August 1989. The fluxes are in units of  $\text{cm}^{-2}\text{s}^{-1}$ .

| $N_\mu / \langle N_\mu \rangle$ | Observed showers | Expected background | Excess (90% C.L.) | Flux (90% CL) $E > 200$ TeV |
|---------------------------------|------------------|---------------------|-------------------|-----------------------------|
| $> 1$                           | 17 577           | 17 687              | $< 173$           | $< 1.1 \times 10^{-13}$     |
| $< 1$                           | 17 611           | 17 793              | $< 154$           | $< 1.0 \times 10^{-13}$     |
| $< 0.3$                         | 1 582            | 1 609               | $< 58$            | $< 3.7 \times 10^{-14}$     |
| $< 0.1$                         | 238              | 244                 | $< 23$            | $< 1.5 \times 10^{-14}$     |

what arbitrary, it would be misleading to choose an energy far from the energy at which the array collects a reasonable fraction of its events. Referring to Fig. 5, we believe a good choice is  $E' = 2 \times 10^{14}$  eV. With this choice of  $E'$ , it turns out that the effective area of the array is quite insensitive to the value of the spectral index  $\beta$ . For example, with  $\beta = 2$  and including showers whose cores lie within 100 m of the center, the effective area of the array exposed to Cygnus X-3 is 7030  $\text{m}^2$ . The corresponding value for  $\beta = 2.7$  (the spectral index of cosmic-ray protons) is 8080  $\text{m}^2$ .

## VI. RESULTS

The data used in this report were taken from 358 live days collected between April 1, 1988 and August 15, 1989. They consist of  $1.5 \times 10^7$  showers with sizes in the range  $3 \times 10^4 < N < 10^6$  and core locations within 100 m of the center of the array.

### A. Limits on the time-averaged radiation from Cygnus X-3

To search for a signal from Cygnus X-3 we use a circular window,  $3^\circ$  radius, on the celestial sphere. When centered on the source, this should contain 72% of the showers from that direction. The distribution of showers in nonoverlapping circles along a strip of declination centered on  $40.9^\circ$ , the declination of Cygnus X-3, is shown in Fig. 6(a). We chose the binning so that the source would be at the center of the middle bin. By averaging the data in the 10 circles adjacent to the source circle we estimated the background to be 35 480 shower from the direction of Cygnus X-3 in 358 transits overhead. During that time we detected 35 188 showers from the source. With 90% confidence<sup>26</sup> the excess over background is less than 197. We can therefore set the following 90%-C.L. upper limit for showers which are *not* muon poor:

$$I(E > 200 \text{ TeV}) < \frac{197}{358 \text{ d} \times 7030 \text{ m}^2 \times 0.72} \\ \approx 1.3 \times 10^{-13} \text{ cm}^{-2}\text{s}^{-1}.$$

There is another way<sup>27</sup> to get this result which does not use the computation of effective area ( $A_{\text{eff}}$ ) described in Sec. V. It uses the known flux of primary cosmic rays above  $2 \times 10^{14}$  eV, which is  $3.5 \times 10^{-9} \text{ cm}^{-2}\text{s}^{-1}\text{sr}^{-1}$ . Our measured limit of 197 showers over a background of 35 480 corresponds to the following 90%-C.L. upper limit for showers which are *not* muon poor:

$$I(E > 200 \text{ TeV}) \\ < \frac{197 \times 3.5 \times 10^{-9} \text{ cm}^{-2}\text{s}^{-1}\text{sr}^{-1} \times 0.0086 \text{ sr}}{35 480 \times 0.72} \\ \approx 2.3 \times 10^{-13} \text{ cm}^{-2}\text{s}^{-1},$$

in a  $3^\circ$  cone collecting 72% of the radiation. Given the uncertainty in the primary flux the agreement between the two methods is satisfactory.

So far we have not used the number of muons in the showers. By cutting on the muon content the background of hadron-induced showers can be reduced by a large factor. For example, including only those showers with less than 10% of the average number of muons for their size produces the distribution shown in Fig. 6(b). With 90% confidence the excess over background is less than 23, which corresponds to an upper limit for showers which *are* muon poor:

$$I(E > 200 \text{ TeV}) < \frac{23}{358 \text{ d} \times 7030 \text{ m}^2 \times 0.72} \\ \approx 1.5 \times 10^{-14} \text{ cm}^2\text{s}^{-1}.$$

The effects of various cuts on the muon content of showers are summarized in Table II. Our exposure in-

TABLE III. A subset of the data shown in Table I taken between May 18 and August 3, 1989. Two intense radio bursts from Cygnus X-3 occurred during this period.

| $N_\mu / \langle N_\mu \rangle$ | Observed showers | Expected background | Excess (90% C.L.) | Flux (90% C.L.) $E > 200$ TeV |
|---------------------------------|------------------|---------------------|-------------------|-------------------------------|
| $> 1$                           | 3679             | 3679                | $< 101$           | $< 3.6 \times 10^{-13}$       |
| $< 1$                           | 3623             | 3689                | $< 75$            | $< 2.8 \times 10^{-13}$       |
| $< 0.3$                         | 288              | 310                 | $< 19.6$          | $< 7.1 \times 10^{-14}$       |
| $< 0.1$                         | 43               | 38.4                | $< 15.3$          | $< 5.5 \times 10^{-14}$       |

cluded the period of two intense radio bursts from Cygnus X-3 which occurred in June and July, 1989. The data taken, during a period of 77 days surrounding these bursts, contain 63.4 transits of the source. They are summarized in Table III.

None of these data show any evidence for radiation from Cygnus X-3. When multiplied by  $E' = 2 \times 10^{14}$  eV to allow a comparison between experiments at different energies our measured limits are generally below the level of signals reported by other observers. (See Table I.)

### B. Search for short-term bursts

We have searched the data for bursts on time scales of 1.0, 0.1, and 0.02 days. The search used nonoverlapping time bins. To estimate the background for these data sets of relatively short duration we use the following method. In the horizontal coordinate frame we take a strip of declination  $\pm 3^\circ$  centered on the declination of Cygnus X-3 and populate each element of hour angle along this strip in proportion to the number of cosmic rays which pass our cuts and come from that part of the sky. The result is shown in Fig. 7. Using this distribution we integrate

the contributions from each element of hour angle weighted by the detector's on-time when Cygnus X-3 is at that hour angle. Standard deviations, calculated from the formula of Li and Ma,<sup>28</sup> are obtained for each time bin using the observed events and expected background. The distributions of standard deviations showed no particularly unusual bursts on any time scale, neither for the total sample nor for the muon-poor sample.

### C. Search for a signal modulated at the 4.79-h period

We find no evidence for such a signal. Our results are shown in Fig. 8. For both ordinary showers and muon-poor showers ( $N_\mu / \langle N_\mu \rangle < 0.1$ ) the light curves are in good agreement with the background which was calculated as follows. For each phase bin, using the distribution of Fig. 7, we integrated the contributions from each element of hour angle weighted by the detector's on-time when Cygnus X-3 is at that hour angle *and* in that phase bin. We have divided our data into subsets of about 3-months duration and varied the trial period from 4.7 to 4.9 h. We find no evidence for a modulation in any of these subsets.

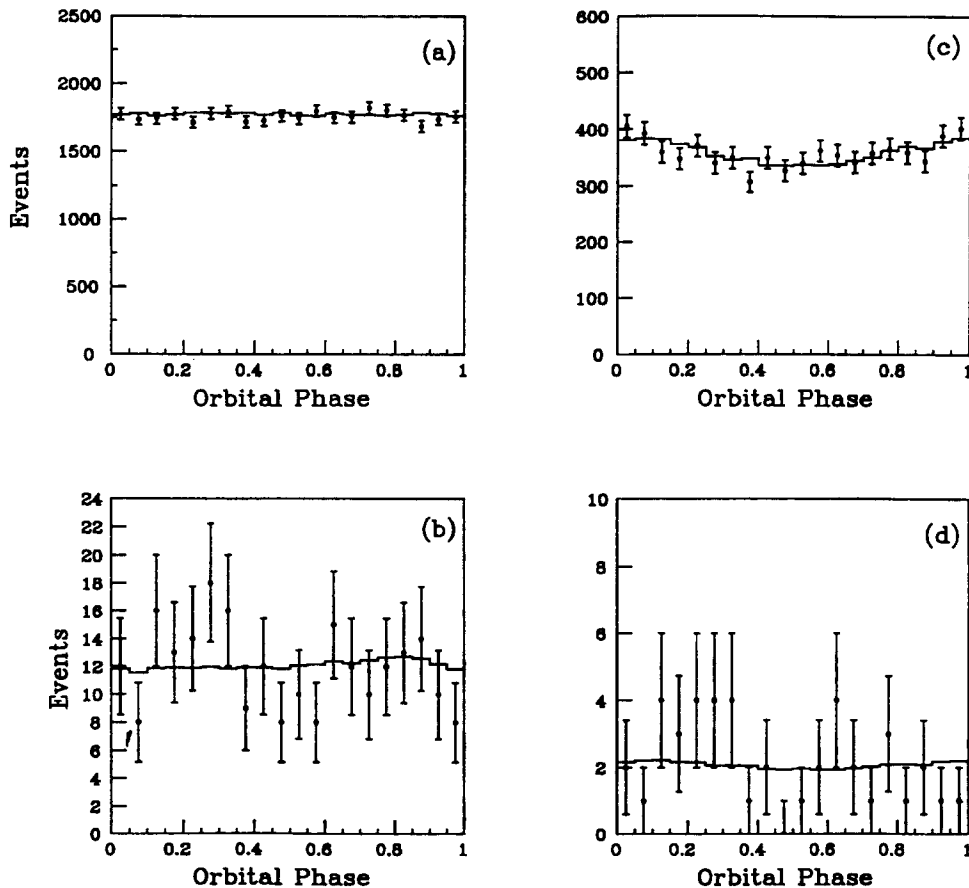


FIG. 8. Light curves for showers coming from the direction of Cygnus X-3. The points with error flags are the data. The solid lines are the calculated backgrounds (see text). (a) All the data; (b) muon-poor showers; (c) all showers in a 77-day period containing the radio flares of June and July 1989; (d) a subset of (c) containing only muon-poor showers. We used the orbital ephemeris of van der Klis and Bonnet-Bidaud (Ref. 29):  $P = 4.792405$  h,  $\dot{P} = 0.9 \times 10^{-9}$ ,  $t_0 = \text{JD}2440949.8962$ . The arrival times were corrected to the bary center.

## ACKNOWLEDGMENTS

The authors gratefully acknowledge the help and support of Colonel Van Prooyen and the staff of Dugway

Proving Grounds. This work was supported in part by the U.S. Department of Energy and the National Science Foundation.

- \*Present address: University of Adelaide, Adelaide, South Australia 5001, Australia.
- †On leave at International Strategic Institute, Stanford University, 320 Galvez Street, Stanford, CA 94305.
- ‡On leave at Istituto Nazionale di Fisica Nucleare, Sezione di Napoli, Mostra d'Oltremare, Padova 20, 80125 Napoli, Italy.
- <sup>1</sup>For review, see W. Hermsen *et al.*, *Astron. Astrophys.* **175**, 141 (1987).
- <sup>2</sup>R. C. Lamb *et al.*, *Astrophys. J. Lett.* **212**, L63 (1977).
- <sup>3</sup>K. Bennett *et al.*, *Astron. Astrophys.* **59**, 273 (1977).
- <sup>4</sup>T. Li and M. Wu, *Astrophys. J.* **346**, 391 (1989).
- <sup>5</sup>Yu. I. Neshpov *et al.*, *Astrophys. Space Sci.* **61**, 349 (1979).
- <sup>6</sup>S. Danaher *et al.*, *Nature (London)* **289**, 568 (1981).
- <sup>7</sup>R. C. Lamb *et al.*, *Nature (London)* **196**, 543 (1982).
- <sup>8</sup>J. C. Douthwaite *et al.*, *Astron. Astrophys.* **126**, 1 (1983).
- <sup>9</sup>M. F. Cawley *et al.*, *Astrophys. J.* **296**, 185 (1985).
- <sup>10</sup>M. Samorski and W. Stamm, *Astrophys. J. Lett.* **268**, L17 (1983).
- <sup>11</sup>J. Lloyd-Evans *et al.*, *Nature (London)* **305**, 784 (1983).
- <sup>12</sup>T. Kifune *et al.*, *Astrophys. J.* **301**, 230 (1986).
- <sup>13</sup>S. C. Tonwar *et al.*, *Astrophys. J.* **330**, L107 (1988).

- <sup>14</sup>B. J. Dingus *et al.*, *Phys. Rev. Lett.* **60**, 1785 (1988).
- <sup>15</sup>G. L. Cassiday *et al.*, *Phys. Rev. Lett.* **62**, 383 (1989).
- <sup>16</sup>M. Teshima *et al.*, *Phys. Rev. Lett.* **64**, 1628 (1990).
- <sup>17</sup>M. A. Lawrence *et al.*, *Phys. Rev. Lett.* **63**, 1121 (1989).
- <sup>18</sup>Y. Matsubara *et al.*, *J. Phys. G* **14**, 385 (1988).
- <sup>19</sup>G. L. Cassiday *et al.*, *Phys. Rev. Lett.* **63**, 2329 (1989).
- <sup>20</sup>R. J. Protheroe, in *Proceedings of the Twentieth International Cosmic Ray Conference*, Moscow, USSR, 1987, edited by V. A. Kozyarivsky *et al.* (Nauka, Moscow, 1987), Vol. 8, p. 21.
- <sup>21</sup>D. Sinclair, *Nucl. Instrum. Methods* **A278**, 583 (1989).
- <sup>22</sup>K. Greisen, *Prog. Cosmic Ray Phys.* **3**, 1 (1956).
- <sup>23</sup>K. Greisen, *Annu. Rev. Sci.* **10**, 63 (1960).
- <sup>24</sup>E. J. Fenyves *et al.*, *Phys. Rev. D* **37**, 649 (1988).
- <sup>25</sup>R. G. Gould and G. P. Schröder, *Phys. Rev.* **155**, 1404 (1967).
- <sup>26</sup>O. Helene, *Nucl. Instrum. Methods* **A212**, 319 (1983); Particle Data Group, R. Gatto *et al.*, *Phys. Lett. B* **204**, 81 (1988).
- <sup>27</sup>This method was suggested by Protheroe (Ref. 20).
- <sup>28</sup>T. Li and Y. Q. Ma, *Astrophys. J.* **272**, 317 (1983).
- <sup>29</sup>M. van der Klis and J. M. Bonnet-Bidaud, *Astron. Astrophys.* **214**, 203 (1989).